Continental J. Applied Sciences
Olasehinde and Ashano (2025) 20 (4): 1 – 33 Doi: 10.5281/zenodo.17352310

Research Article

Multi-Scale Element Interdependency in Mineral Exploration: Integral Transform-Based Cross-Variogram Modeling of Geochemical Data from the Riruwai Complex

Adeyinka Olasehinde[1*] and Edafetano C. Ashano[2]
[1]Department of Geology, Gombe State University, [2]Department of Geology, University of Jos
*Corresponding author: yinka@gsu.edu.ng

Abstract

Geostatistical methods are fundamental for characterizing the spatial distribution and interdependencies of geochemical elements, providing crucial insights for mineral exploration. This paper investigates the application of integral transform approaches, specifically Normal Score Transformation, Fourier Transform, and Wavelet Transform, to cross-variogram modeling of geochemical data. We delineate the theoretical underpinnings and interpretation of cross-variograms, emphasizing how their parameters directly inform exploration strategies. The advantages and limitations of these integral transforms in addressing common challenges such as highly skewed data distributions, outliers, and multi-scale spatial heterogeneity are thoroughly discussed. Utilizing a conceptual framework applied to Riruwai geochemical dataset, comprising 39 diverse samples across multiple lithological units, we emphasize the critical role of rigorous data preprocessing, geological domaining, and the strategic selection of geologically relevant element pairs. Elemental pairs such as Fe_2O_3–MgO, Sr–Ba, and U–Th demonstrated co-regionalization patterns consistent with magmatic differentiation, hydrothermal alteration, and metallogenic processes. This work demonstrates how these advanced geostatistical techniques can significantly enhance the robustness of variogram models, leading to more accurate resource estimation, improved target generation, and reduced exploration uncertainty, particularly in complex geological settings with irregularly spaced data.

Keywords: Cross-Variogram Modeling, Integral Transforms, Geochemical Data Analysis, Mineral Exploration, Riruwai Younger Granite Complex

Received: 13 May 2025 **Accepted: 21 September 2025**

ISSN: 3043–6087. Science and Education Development Inst., Nigeria

Introduction

1. Introduction to Geostatistical Modeling and Spatial Dependence in Mineral Exploration

Geostatistics, a specialized branch of statistics, is fundamentally dedicated to the analysis and interpretation of spatially or spatiotemporally correlated datasets (Goovaerts, 1997; Chiles & Delfiner, 2012). In the context of mineral exploration, its core purpose lies in quantifying spatial dependence, which enables robust prediction, estimation, and simulation of regionalized variables such as ore grades or pathfinder element concentrations across a given geological domain (Journel & Huijbregts, 1978; Wackernagel, 2003). This understanding is paramount for a diverse array of applications, ranging from the precise estimation of mineral resources to critical environmental monitoring and assessment associated with mining activities (Thayer et al., 2003)

At the heart of geostatistical modeling is the characterization of spatial autocorrelation. This fundamental concept describes the inherent tendency for values at nearby locations to exhibit greater similarity than those situated farther apart (Matheron, 1965). Such a non-random distribution is a pervasive characteristic of natural phenomena, including the spatial variability of geochemical concentrations or the grades of mineral deposits. The quantification of this spatial autocorrelation is typically achieved through the use of variograms (Chilès & Delfiner, 2012; Isaaks & Srivastava, 1989). The variogram serves as a foundational tool in geostatistics, providing a quantitative measure of the spatial dependence or autocorrelation of a single regionalized variable. It is conventionally depicted as a graph that illustrates the average squared difference between pairs of data points as a function of their separation distance, commonly referred to as the lag. Extending this univariate concept, the cross-variogram measures the spatial dependence between two different regionalized variables. This powerful tool provides a quantitative measure of how two distinct variables co-vary in space.

Cross-variograms are pivotal for analyzing spatial relationships within multivariate contexts, finding widespread application in multivariate geostatistical modeling, spatial prediction techniques such as cokriging, and various simulation methodologies (Journel & Huijbregts, 1978; Wackernagel, 2003). They offer profound insights into the underlying spatial structure and the intricate interdependencies that exist among multiple variables. The emphasis on cross-variograms in geochemical analysis for mineral exploration stems from a recognition of the inherent interconnectedness of geochemical processes. Geochemical elements are rarely isolated entities within the Earth's crust; rather, they are integral components of complex, interconnected systems governed by a multitude of geological processes such as magmatic differentiation, hydrothermal alteration, or surficial weathering (Rollinson, 1993; Reimann & Filzmoser, 2000). Consequently, the spatial co-variability observed through cross-variograms acts as a direct fingerprint of these underlying processes. For instance, a strong positive spatial correlation between elements like copper and molybdenum might signify a specific type of porphyry mineralization, whereas a negative correlation between silica and iron could indicate a silicification front or an argillic alteration zone. This perspective suggests that the judicious selection of element pairs for cross-variogram analysis should be guided by geological hypotheses concerning their genetic relationships be it co-precipitation, antagonistic behavior, or a common source rather than relying solely on empirical statistical correlation. This approach transforms statistical analysis into a potent tool for inferring and mapping geological processes, enriching the geological model with quantitative spatial relationships crucial for exploration targeting.

Furthermore, relying exclusively on univariate variograms for individual geochemical elements in a complex geological environment would yield an incomplete and potentially misleading understanding of the overall system. Geochemical systems are inherently multivariate; elements interact chemically and physically, and their distributions are frequently controlled by common underlying factors. The cross-variogram, therefore, transcends being merely an advanced analytical option; it emerges as a fundamental requirement for adequately capturing the true spatial complexity and interdependencies of geochemical processes (Chiles & Delfiner, 2012). This leads to the development of more comprehensive and robust models for critical applications such as mineral resource estimation or environmental risk assessment, as it intrinsically accounts for the multi-element nature of geological formations and the intricate processes that shaped them. Ultimately, this translates to more effective and efficient mineral exploration strategies.

2. Riruwai Geochemical Data Overview and Exploration Significance

The geochemical dataset under consideration comprises analyses from 39 distinct samples, systematically labeled B3, B4, B6, B7, DS1, DS2, GR2, Y1, Y2, Y3, Y4, Y5, Y7, Y7A, Y15, Y18, Y24, Y26, Y27, Y29, Y30, Y32, Y33, Y34, Y34B, Y35, Y36, Y37, Y38, Y39, Y41, Y42, Y44, Y45, Y49, ZB1, ZB2, ZB3, and ZB4. Each of these samples is precisely associated with geographic coordinates (Latitude and Longitude), establishing their explicit spatial context, which is fundamental for any subsequent geostatistical analysis. For instance, sample B3 is located at 10.729556 N, 8.710947E. The samples are broadly categorized into several lithological units: "Medium Grained Biotite Granite" (B3, B4, B6, B7), "Fine Grained Biotite Granite" (Y2, Y3, Y4, Y5), "Ignimbrites" (DS1, DS2), "Undifferentiated Rhyolites" (GR2, Y24, Y26), "Breccia" (Y1), "Alkaline Rhyolite" (Y7, Y15, Y30), "Rhyolite"

ISSN: 3043–6087. Science and Education Development Inst., Nigeria

(Y7A, Y18, Y34, ZB2, ZB3), "Porphritic Rhyolite" (Y27, Y29, ZB4), "Pyroxene Fayalite Granite Porphyries" (Y32, Y33, ZB1), "Kaffo river Riebeckite Porphyry" (Y34B, Y37), "Early Rhyolite" (Y35, Y36), "Advedsonite Microgranite" (Y38, Y39), "Kaffo albite Arfvedsonite Granite" (Y41, Y42, Y44), and "Aegirine Arfvedosonite Granite" (Y45, Y49). This lithological diversity is of paramount importance in mineral exploration, as different rock types inherently possess distinct geochemical signatures and are expected to exhibit varying spatial behaviors due to their unique petrogenetic histories and alteration susceptibility. The dataset provides a comprehensive suite of both major oxide concentrations (e.g., SiO_2, CaO, MgO, K_2O, Na_2O, TiO_2, MnO, P_2O_5, Fe_2O_3, Al_2O_3, LOI, Total, A/CNK) and a wide range of trace element concentrations (e.g., V, Cr, Cu, Sr, Zr, Ba, Zn, Ce, Pb, Sn, Ga, Y, Ni, Rb, Nb, Eu, Mo, Co, Ta, W, Hf, Gd, U, Th, Nd, REE, LREE/HREE,Y). This rich compositional information forms a robust foundation for thoroughly exploring elemental interrelationships and their spatial distributions, which can directly indicate mineralization.

A preliminary review of the dataset reveals characteristics that are highly pertinent to geostatistical analysis, particularly the potential for skewed distributions and the presence of outliers. Geochemical data, especially for trace elements and those linked to mineralization, frequently exhibit highly skewed distributions, often approximating log-normal or power-law behaviors, and can contain significant extreme values or outliers. The provided data shows substantial variations across samples for elements such as Cr, Sr, Ba, Zn, Ga, Ni, Eu, Co, Ta, U, Nd, REE, and LREE/HREE,Y, particularly when comparing different lithological series. This pronounced variability strongly suggests that data transformation, such as Normal Score Transformation, will likely be a necessary preprocessing step to ensure robust variogram modeling, which is crucial for reliable resource estimation. The presence of numerous distinct rock types within the dataset further indicates the potential for non-stationarity or multi-modal distributions. In such scenarios, geochemical characteristics and their spatial continuity might vary significantly between these distinct geological domains, necessitating careful consideration during the modeling process.

To provide a concise overview of the dataset, Table 1 summarizes key statistics and the converted spatial coordinates for a selection of the Riruwai geochemical samples. This table facilitates immediate comprehension of the data's scale, variability, and spatial extent, and provides the necessary decimal degree coordinates for spatial distance calculations in variogram analysis. The inclusion of summary statistics for selected elements highlights their range, central tendency, and dispersion, which are vital for anticipating potential issues like high skewness or the presence of outliers, thereby informing the decision to apply integral transforms for robust exploration modeling.

ISSN: 3043–6087. Science and Education Development Inst., Nigeria

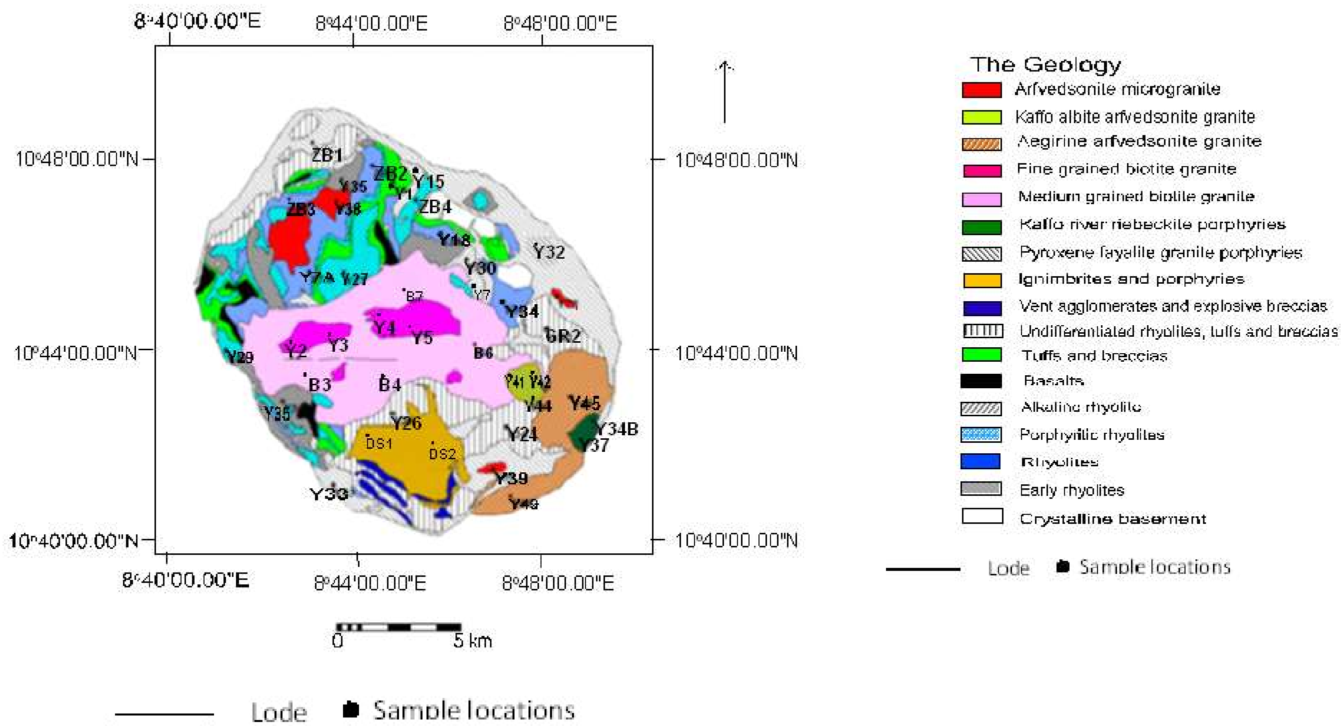

Figure 1. The Geological Map of the Riruwai Complex with the Sample Points used for Geochemical Analysis (modified after, Ogunleye et al., 2006)

Table 1: Summary Statistics and Coordinates of Selected Riruwai Geochemical Samples

Sample ID	Lithology	Latitude (Decimal Degrees)	Longitude (Decimal Degrees)	SiO_2 (%)	Fe_2O_3 (%)	Cr (ppm)	Sr (ppm)	REE (ppm)	LOI (%)	Total (%)
B3	Medium Grained Biotite Granite	10.729556	8.710947	75.20	2.39	0.02	33.00	294.36	2.31	99.99
B4	Medium Grained Biotite Granite	10.728833	8.736086	75.78	1.47	0.01	48.00	344.64	1.77	99.29
B6	Medium Grained Biotite Granite	10.735167	8.752728	76.29	1.45	0.04	37.00	308.82	1.87	99.92
B7	Medium Grained	10.751108	8.769411	75.29	2.35	0.04	44.00	304.65	1.87	99.86

	Biotite Granite									
Y4	Fine Grained Biotite Granite	10.745167	8.733081	76.01	12.34	220.00	4750.00	2.64	1.69	100.37
Y5	Fine Grained Biotite Granite	10.742944	8.741714	73.30	13.22	190.00	1120.00	4.86	1.58	99.76
Y3	Fine Grained Biotite Granite	10.737714	8.704558	74.80	1.35	0.06	11.32	442.26	2.48	100.76
Y2	Fine Grained Biotite Granite	10.739953	8.715817	73.30	2.22	0.07	11.35	480.22	3.40	100.38
DS1	Ignimbrites	10.705067	8.725983	75.45	1.97	0.06	11.10	405.38	2.10	100.79
DS2	Ignimbrite	10.703228	8.745125	74.41	1.19	0.01	12.10	429.07	1.92	98.91
GR2	Undifferntiated Rhyolites	10.752861	8.781872	72.10	3.39	0.09	11.00	505.09	2.30	100.27
Y1	Breccia	10.793797	8.734164	72.80	2.13	0.01	11.78	360.35	4.02	100.56
Y7	Alkaline Rhyolite	10.755214	8.715817	76.21	2.09	0.04	81.70	432.55	0.75	100.30
Y7A	Rhyolite	10.745167	8.733081	72.60	1.32	0.04	11.56	243.56	3.86	99.79
Y15	Alkaline Rhyolite	10.794169	8.734161	74.07	2.20	0.06	12.22	310.44	2.48	100.16
Y18	Rhyolite	10.769306	8.745822	73.90	2.83	0.01	11.44	311.91	1.16	99.98
Y24	Undifferntiated Rhyolites	10.712158	8.772894	76.30	2.40	0.09	12.60	334.47	2.66	100.80
Y26	Undifferntiated Rhyolites	10.713244	8.736861	74.90	1.29	0.01	12.45	325.65	2.50	100.78
Y27	Porphritic Rhyolite	10.759633	8.721053	72.45	1.64	0.07	13.44	389.44	2.04	99.19
Y29	Porphritic Rhyolite	10.729533	8.690567	74.30	2.24	0.06	12.34	256.61	1.84	100.94
Y30	Alkaline Rhyolite	10.763375	8.756714	76.45	1.66	0.02	13.01	492.07	0.86	100.65
Y32	Pyroxene fayalite Granite Porphyries	10.749650	8.771364	76.53	1.51	0.01	18.20	425.50	0.76	100.72
Y33	Pyroxene Fayalite Granite Porphyries	10.692433	8.712483	76.01	2.81	0.04	14.03	440.37	0.77	101.53
Y34	Rhyolite	10.749650	8.771364	71.07	3.29	0.04	20.31	454.63	2.60	99.68
Y34B	Kaffo river Riebeckite Porphyry	10.709194	8.796167	74.60	2.95	0.06	16.34	358.20	1.01	99.40
Y35	Early Rhyolite	10.718781	8.703081	74.10	2.02	0.01	14.55	409.69	1.41	98.06

Y36	Early Rhyolite	10.780411	8.708272	73.53	2.24	0.09	12.00	400.05	1.20	99.79
Y37	Kaffo River Riebeckite Porphyry	10.704375	8.791903	74.40	2.43	0.01	19.00	480.94	1.41	99.67
Y38	Advedsonite Microgranite	10.755600	8.783747	74.70	2.09	0.07	17.60	466.82	1.03	99.75
Y39	Advedsonite Microgranite	10.697303	8.765022	74.50	2.21	0.06	16.32	467.17	0.24	100.05
Y41	Kaffo albite Arfvedsonite Granite	10.745167	8.733081	72.20	2.41	0.02	11.00	754.22	1.68	99.03
Y42	Kaffo Albite Arfvedsonite Granite	10.725525	8.710725	73.54	2.36	0.04	9.45	627.42	1.34	99.59
Y44	Kaffo Albite Arfvedsonite Granite	10.720328	8.777392	74.50	2.33	0.04	6.21	679.03	1.84	99.67
Y45	Aegirine Arfvedosonite Granite	10.726278	8.791650	76.81	1.26	0.03	7.43	484.41	0.72	99.90
Y49	Aegirine Arfvedosonite Granite	10.687283	8.771786	76.43	2.31	0.02	4.01	446.25	0.89	99.84
ZB1	Pyroxene Fayalite Granite Porphyries	10.801203	8.712381	73.72	2.51	0.01	5.00	326.37	1.60	99.28
ZB2	Rhyolite	10.792678	8.728908	75.50	2.34	0.03	13.00	362.08	0.48	99.87
ZB3	Rhyolite	10.779667	8.707144	74.60	2.72	0.03	13.04	464.46	1.76	100.46
ZB4	Porphritic Rhyolite	10.793428	8.736417	73.11	2.98	0.01	13.52	424.32	1.03	100.50
Statistics (All 39 Samples)										
Mean				74.51	2.72	10.55	197.29	416.03	1.72	100.01
Median				74.50	2.24	0.04	13.01	405.38	1.69	99.92
Min				71.07	1.19	0.01	4.01	2.64	0.24	98.06
Max				76.81	13.22	220.00	4750.00	754.22	4.02	101.53
Std Dev				1.43	2.44	45.93	792.83	140.08	0.87	0.66
Range				5.74	12.03	219.99	4745.99	0.87	3.78	3.47
Coefficient of Variation (%)				1.92	89.71	435.36	463.33	0.66	50.58	0.66

3. Fundamentals of Cross-Variogram Analysis and Exploration Insights

The cross-variogram stands as a fundamental geostatistical measure that quantifies the spatial dependence between two distinct regionalized variables, denoted as:

$Z_1(x)$ and $Z_2(x)$, at different spatial locations x (Goovaerts, 1997; Wackernagel, 2003). It represents a crucial extension of the traditional variogram, which primarily focuses on the spatial autocorrelation of a single variable (Chilès & Delfiner, 2012). Mathematically, the cross-variogram $\gamma_{12}(h)$ between two variables $Z_1(x)$ and $Z_2(x)$ at locations x and x+h is defined as half the expected value of the product of their differences over a separation distance h

$$\gamma_{12}(h) = \frac{1}{2}\mathrm{E}[Z_1(\mathrm{x}) - Z_1(\mathrm{x}+\mathrm{h})][Z_2(\mathrm{x}) - \mathrm{Z}_2(x+h)] \qquad (1)$$

This formulation effectively captures the spatial covariance between Z_1 and Z_2 as a function of their spatial separation and E denote expected values (Goovaerts, 1997)

Key properties of the cross-variogram ensure its validity and analytical utility in geostatistics:

(a) Symmetry: The cross-variogram is symmetric, such that

$$\gamma_{12}(h) = \gamma_{21}(h) \qquad (2)$$

This implies that the directional spatial relationship is mutual between the variables (Chilès & Delfiner, 2012).

(b) Positive Definiteness**:** The matrix composed of auto-variograms and cross-variograms must be positive definite to ensure that the resulting covariance matrix used in kriging is invertible and yields valid estimation variances (Wackernagel, 2003).

(c) Boundedness: The absolute value of the cross-variogram is bounded by the geometric mean of the auto-variograms of the individual variables:

$$|\gamma_{12}(\mathrm{h})| \leq \sqrt{\gamma_{11}(\mathrm{h})\gamma_{22}(\mathrm{h})} \qquad (3)$$

This condition ensures internal consistency in the spatial model (Goovaerts, 1997).

A related concept, the pseudo-cross-variogram, is defined as half the variance of the difference between two variables at corresponding spatial locations. It is useful for assessing spatial dissimilarities and typically approaches zero as the distance tends toward zero (Myers, 1982).

Constructing and modeling cross-variograms involves three primary stages: data preparation, empirical cross-variogram calculation, and theoretical model fitting (Isaaks & Srivastava, 1989; Wackernagel, 2003). The empirical or experimental cross-variogram is computed using the following formula:

$$\gamma_{12}(h) = \frac{1}{2N(h)} \sum_{i=1}^{N(h)} Z_i(x_i) - Z_1\,(x_i + h) Z_2(x_i) - Z_2(x_i + h) \tag{4}$$

where N(h) is the number of data pairs separated by lag h (Chilès & Delfiner, 2012). Variants of this calculation include: Directly applying the formula, reduces the influence of outliers (Cressie, 1993) and uses of kernel-based techniques, suitable when data do not meet parametric assumptions (Lark, 2000). Proper data preparation is essential prior to modeling and includes verifying spatial coordinates, removing or imputing missing values, and treating outliers (Goovaerts, 1997).

The experimental cross-variogram plot visually expresses the spatial dependence between variables, interpreted through three critical parameters:

(a) Nugget Effect

This quantifies variability at very short distances and often reflects sampling error, measurement noise, or micro-scale heterogeneity (Isaaks & Srivastava, 1989). In mineral exploration, a high nugget effect can indicate erratic mineralization or unresolved geological features, such as coarse gold distribution, necessitating denser sampling (Cameron et al., 2004).

(b) Sill

The sill marks the plateau of the variogram, beyond which no further increase in dissimilarity occurs. For geochemical elements, it reflects the maximum spatial dissimilarity or covariance. A distinct sill facilitates reliable spatial modeling and indicates a strong spatial structure (Wackernagel, 2003).

(c) Range

This is the distance beyond which spatial correlation ceases. It determines the "radius of influence" in Kriging and directly influences drill spacing or sampling strategy (Journel & Huijbregts, 1978). A small range suggests tightly localized features (e.g., narrow veins), while a large range indicates broader, continuous mineralized zones or alteration halos.

Table 2: Interpretation of Cross-Variogram Parameters and Exploration Implications

Parameter	Definition (Geostatistical Theory)	Geochemical Interpretation	Implication for Mineral Exploration
Nugget Effect	Variability at very small distances, including the origin; attributed to measurement error or small-scale spatial variations.	Quantifies combined analytical/sampling error and inherent geological heterogeneity below sampling resolution (e.g., micro-scale mineralogical variations, localized alteration).	High nugget suggests erratic mineralization or fine-scale heterogeneity, requiring denser sampling to resolve. Informs sampling strategy and confidence in short-range estimates.
Sill	The maximum variability between two variables; the point at which spatial correlation no longer increases with distance.	Represents the maximum level of spatial covariance or dissimilarity between two elements as their separation distance increases.	Indicates the overall strength of the spatial relationship. A higher sill (relative to the nugget) implies a strong, modelable spatial structure, leading to more reliable resource estimates.
Range	The distance beyond which variables are no longer spatially correlated.	Defines the characteristic spatial scale of the geological process responsible for the elements' co-variation (e.g., extent of hydrothermal alteration, magmatic differentiation zone).	Crucial for optimal drill hole spacing and delineating the spatial extent of mineralization or alteration zones. Defines the "radius of influence" for Kriging, guiding target generation.

A substantial nugget effect in geochemical cross-variograms carries dual implications: (i) it quantitatively captures analytical and sampling uncertainties, and (ii) it may signify meaningful geological variability at scales smaller than the sample support (Reimann &

ISSN: 3043–6087. Science and Education Development Inst., Nigeria

Filzmoser, 2000). For instance, in a gold-silver system, a large nugget may point to fine-scale controls such as discrete sulfosalt patches or selective mineral trapping in microfractures.

Likewise, the range in a cross-variogram reveals the spatial scale of geological processes. A 100-meter range between arsenic and gold, for example, indicates that mineralizing fluids likely influenced geochemistry within that radius thus informing the extent of potential mineralization footprints (Perret et al., 2021).

Table 2 provides a concise summary of these critical cross-variogram parameters, offering their definitions, their specific interpretation within the geochemical domain, and their implications for subsequent spatial modeling efforts in mineral exploration.

A typical cross-variogram plot illustrates the spatial dependence between two variables. The Y-axis represents the semivariance (a measure of dissimilarity), and the X-axis represents the lag distance (separation distance between sample pairs).

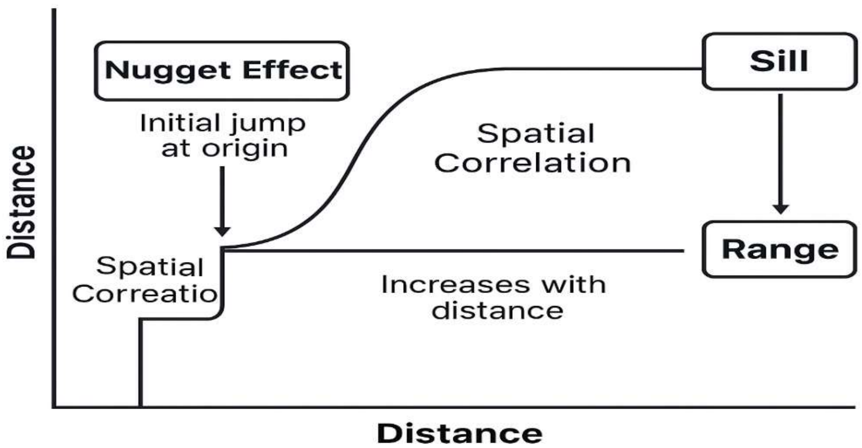

Figure 2: Conceptual Cross-Variogram Plot illustrating the Nugget Effect, Sill, and Range. The X-axis represents Lag Distance (h), and the Y-axis represents Semivariance (γ(h)). The nugget represents variability at the origin, the semivariance increases with distance, leveling off at the sill, and the range is the distance beyond which variables are no longer spatially correlated.

The variogram is a special case of the cross-variogram, applying when both variables are identical (i.e., Z_1=Z_2) (Wackernagel, 2003).

The cross-variogram is intrinsically linked to other fundamental geostatistical concepts (Figure 3), forming a coherent framework for spatial analysis. The cross-variogram generalizes this concept by measuring spatial co-dependence between different variables, such as copper and molybdenum. Both the variogram and cross-variogram are mathematically linked to the covariance function, which directly expresses spatial similarity rather than dissimilarity. These tools underpin advanced geostatistical modeling techniques like cokriging, which utilizes multiple spatially correlated variables to improve estimation precision for under-sampled primary variables (Myers, 1982; Goovaerts, 1997). This interrelationship is essential when integrating pathfinder elements and structural proxies in mineral exploration workflows.

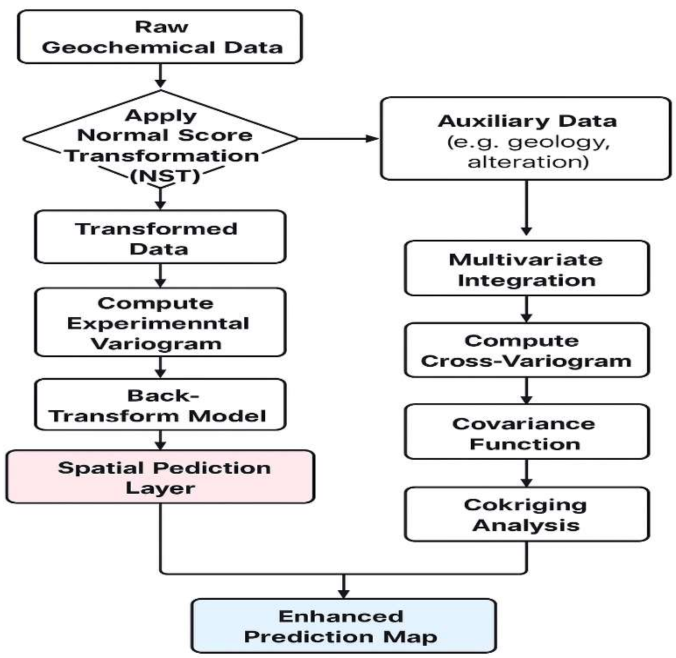

Figure 3: Relationships between key geostatistical tools. The Variogram is a special case of the Cross-Variogram (for a single variable), and the Cross-Variogram is related to the Covariance Function. Both are fundamental for advanced spatial prediction techniques like Cokriging.

Figure 4 visually distinguishes between spatially structured data and random noise, and how their respective variograms would appear. This conceptual diagram distinguishes between two spatial data regimes:

(a) Left (structured**):** Spatially correlated data show a pattern where nearby values are similar, resulting in a variogram with: Low nugget, gradual increase in semivariance with distance, and well-defined sill and range (Isaaks & Srivastava, 1989).
(b) Right (random): Random data lack spatial structure. The resulting variogram: Shows a large nugget effect, reaches sill quickly (if at all), indicates no meaningful spatial continuity.

This comparison is crucial in geochemical exploration. For instance, structured variograms suggest mineralizing processes governed by coherent geological controls (e.g., hydrothermal flow), whereas random patterns may point to transported anomalies, post-depositional alteration, or analytical noise (Reimann & Filzmoser, 2000).

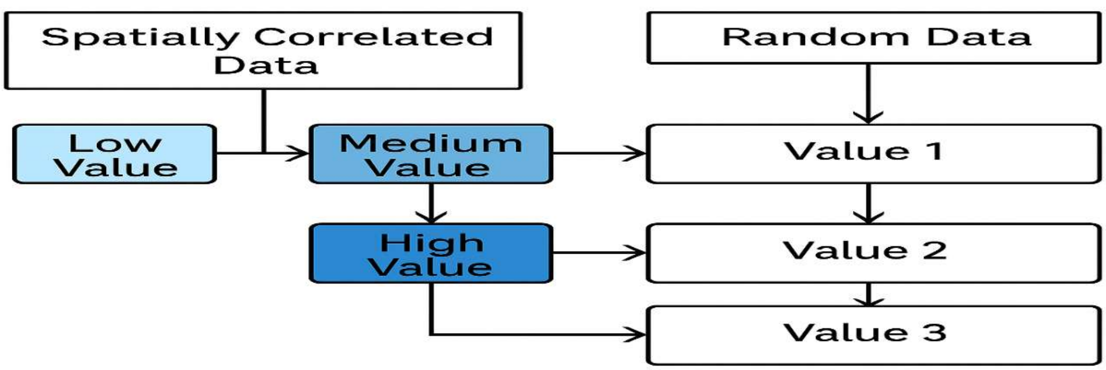

Figure 4: Conceptual Illustration of Spatial Correlation vs. Randomness. Spatially correlated data (left) exhibit a clear pattern, resulting in a variogram with a low nugget and well-defined sill and range. Random data (right) show no discernible pattern, leading to a variogram dominated by a high nugget effect, indicating a lack of spatial structure.

Anisotropy in Geostatistical Modeling: Implications for Mineral Exploration
Anisotropy is a fundamental concept in geostatistics that describes the condition where spatial dependence varies with direction. In the context of geological datasets, anisotropy is a prevalent and critical characteristic that significantly influences the accuracy and reliability of spatial modeling. Figure 5 conceptually illustrates this phenomenon,

ISSN: 3043–6087. Science and Education Development Inst., Nigeria

showing how spatial continuity differs depending on the orientation of sampling or geological features.

Geological anisotropy is typically directional that is, mineralization and associated geochemical signatures exhibit greater spatial continuity along certain geological directions. This is especially evident along strike, where mineralized bodies such as veins, shear zones, or stratiform deposits extend with relative uniformity. In contrast, spatial continuity is generally weaker across strike or down dip, where geological discontinuities, lithological changes, or structural offsets may disrupt continuity over shorter distances (Chilès & Delfiner, 2012).

This directional behavior necessitates the use of directional variograms, where variograms are computed along multiple azimuths (e.g., 0°, 45°, 90°, 135°) to detect and quantify the directional variation in spatial correlation. These directional variograms reveal whether anisotropy exists and allow the geostatistician to model it appropriately within the variogram structure. Two primary types of anisotropy are commonly encountered:

1. **Geometric Anisotropy**: This occurs when the sill remains constant in all directions, but the range varies. In such cases, spatial correlation persists over longer distances in one direction than another, although the overall variance (sill) remains the same. This type of anisotropy is often associated with elongated geological features like dikes or mineralized veins.
2. **Zonal Anisotropy**: In this form, both the range and the sill vary with direction. This indicates not only that spatial continuity differs across orientations, but also that the total variability changes—a situation that might arise from differing lithological controls or varying intensity of mineralizing processes in different directions (Wackernagel, 2003).

Accounting for anisotropy during variogram modeling is essential for producing accurate spatial predictions and unbiased resource estimates. Failure to address anisotropy can result in misleading variogram models, which in turn yield biased kriging estimations or inefficient sampling strategies. For example, if a mineral deposit is strongly anisotropic along strike, using an isotropic model (which assumes equal continuity in all directions) may underestimate resource extent or lead to improper drill hole placement.

In mineral exploration, especially within structurally controlled deposits, anisotropy often governs the orientation and geometry of ore bodies. By incorporating anisotropic variogram models, geoscientists and resource estimators can more accurately capture the

ISSN: 3043–6087. Science and Education Development Inst., Nigeria

spatial behavior of mineralization, leading to more robust interpretations and effective exploration targeting (Madani et al., 2022). Moreover, accounting for anisotropy enhances the realism of geostatistical simulations and ensures that interpolation methods like kriging reflect the true geological architecture.

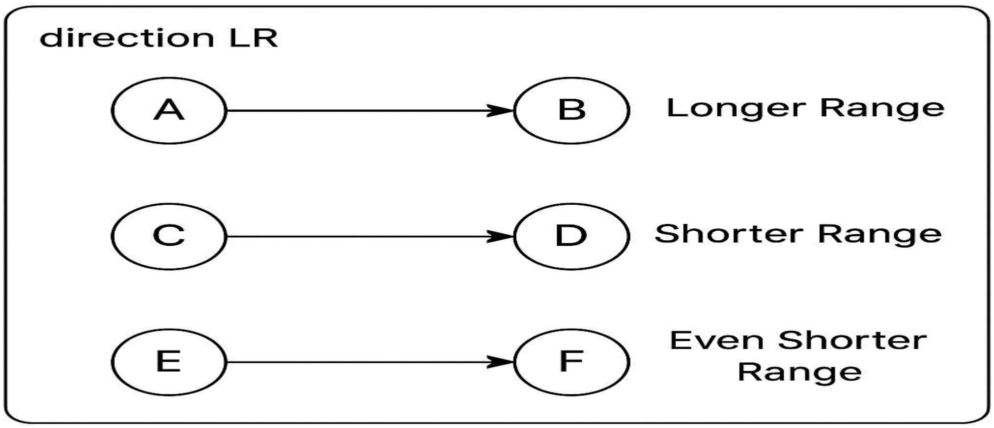

Figure 5: Conceptual Diagram of Anisotropy in Variograms. Anisotropy indicates that spatial continuity varies with direction. This is often observed in geological settings, where mineralization or geological features may extend further in one direction (e.g., along strike) than across another (e.g., across dip or vertically), leading to different variogram ranges for different orientations.

4. Integral Transforms for Variogram Modeling: Theory and Application in Mineral Exploration

Integral transforms are powerful mathematical tools used to map functions from their original domain into a new domain, where operations such as differentiation, integration, and convolution become algebraically simpler. These transformations are widely utilized in various fields, including signal processing, physics, and, importantly, geostatistics (Bracewell, 2000). In geostatistical modeling, especially for mineral exploration, certain integral transforms are particularly effective in managing the challenges posed by skewed, non-Gaussian spatial data. One of the most widely applied transformations in this context is the Normal Score Transformation (NST).

Normal Score Transformation for Robust Resource Estimation

Many geostatistical estimation techniques, such as Ordinary Kriging and Sequential Gaussian Simulation, are fundamentally built on the assumption that input data follow a multivariate Gaussian (normal) distribution (Goovaerts, 1997, Boisvert & Deutsch, 2011). However, in mineral exploration, geochemical datasets particularly those involving trace

ISSN: 3043–6087. Science and Education Development Inst., Nigeria

elements or pathfinder elements associated with mineralization often exhibit highly skewed distributions. These may include log-normal, power-law, or mixed distributions and frequently contain extreme values or statistical outliers (Journel & Huijbregts, 1978; Verly, 1993). Such departures from normality can distort experimental variograms, producing structures that are noisy, difficult to interpret, and challenging to model with theoretical variogram functions (Deutsch & Journel, 1998). Traditional corrective measures, such as capping extreme values or data trimming, are simplistic and risk discarding valuable geochemical information. In contrast, Normal Score Transformation (NST) provides a more mathematically robust and interpretable alternative. NST transforms the cumulative distribution function (CDF) of the original data into that of a standard Gaussian distribution while preserving the rank order of data values. This process involves computing the empirical CDF of the raw data, assigning each value a quantile, and then mapping this quantile to its equivalent in the standard normal distribution (Wang et al., 2007). This transformation reduces the disproportionate influence of high-value outliers and cluster effects, making the resulting variograms significantly more structured and smooth, thereby enhancing the ability to fit reliable models.

A common approach to implementing NST involves using Hermite polynomials, which model the transformation function. These polynomials (often up to the 30th order) approximate the relationship between raw and normal scores (Deutsch & Journel, 1998). The accuracy of this transformation is often evaluated using a Hermite fit graph, which visually compares the empirical and theoretical CDFs. Notably, negative values in raw datasets, which may lack physical meaning (e.g., negative concentrations), are typically clamped at zero before transformation to ensure mathematical validity. Once transformed, the experimental variogram is computed in the Gaussian domain. The fitted variogram in this space generally exhibits more coherent structures with a clearly defined nugget, sill, and range, which are essential for spatial modeling. However, it is crucial to recognize that the transformed variogram parameters especially the sill and nugget are often "optimistic," reflecting reduced variance due to transformation rather than actual geological variability. As such, back-transformation is required before applying kriging or simulation models in the original data space (Goovaerts, 1997; Chilès & Delfiner, 2012).

This multi-step process introduces a methodological trade-off in mineral resource estimation. While NST enables effective variogram modeling, it complicates direct interpretation because estimation must ultimately occur in the raw data space. The back-transformation step is not trivial, as it requires inverse mapping of estimated normal scores to their corresponding raw values, an operation sensitive to the quality of the initial transformation and the data distribution. Despite these complexities, NST is almost

ISSN: 3043–6087. Science and Education Development Inst., Nigeria

indispensable in modern geostatistical workflows (Figure 6), particularly for highly skewed geochemical datasets. Its use results in more robust spatial models, reducing estimation bias and improving the geological plausibility of resource models. As such, practitioners must be keenly aware of the transformation space in which variograms are modeled versus the domain of final estimation, and clearly communicate the assumptions and limitations of the transformation to stakeholders in resource reporting and decision-making.

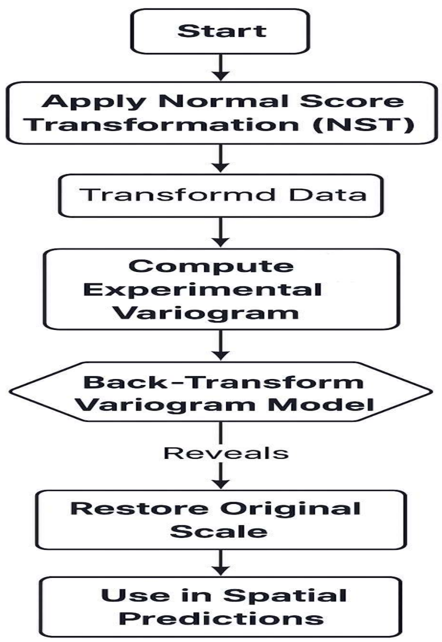

Figure 6: Workflow for Normal Score Transformation in Variogram Modeling. Raw, often skewed, geochemical data are transformed to a Gaussian distribution, allowing for more robust variogram modeling. The fitted model is then back-transformed for use in estimation and simulation in the original data space.

Fourier Transform for Identifying Structural Controls on Mineralization

The Fourier Transform (FT) offers a powerful mathematical bridge between the spatial and frequency domains, making it invaluable for understanding structural controls in mineral exploration (Figure 7). In geostatistics, the spatial periodogram provides a non-parametric estimate of spectral density, which is essentially the Fourier Transform of the autocovariance function of a spatial process (Fuentes, 2007). This spectral density function, denoted $fZ(\omega)$, is intimately related to the autocovariance function $cZ(x)$

ISSN: 3043–6087. Science and Education Development Inst., Nigeria

through the Fourier Transform, and vice versa, with the covariance function recoverable via inverse transformation (Priestley, 1981). This mathematical symmetry underlies the analytical power of spectral techniques in spatial modeling.

When applied to spatial datasets, a semi-variogram can be derived by transforming spatial data into the frequency domain. The standard approach involves removing the DC component (the mean), multiplying the transformed signal by its complex conjugate, and applying an inverse Fourier Transform (Isaaks & Srivastava, 1989). The widespread adoption of the Fast Fourier Transform (FFT) has drastically improved computational efficiency, reducing complexity from $O(N^2)$ to $O(N \log N)$, particularly when data lengths are powers of two (Briggs & Henson, 1995). Modern algorithms have further advanced to handle large datasets of arbitrary length (Frigo & Johnson, 2005), making Fourier methods increasingly applicable in geostatistical workflows, particularly in analyzing geophysical or remote sensing data.

One of the principal advantages of using Fourier methods lies in the asymptotic uncorrelation of spectral estimates at distinct Fourier frequencies (Fuentes, 2007). This contrasts with variogram estimates in the spatial domain, which are often correlated due to shared data points across lag distances. The reduced correlation structure of the spectral domain facilitates more robust statistical inference, such as through nonlinear least squares fitting. Additionally, spectral techniques allow for noise suppression by employing smoothing filters or data tapers (e.g., Hamming or Blackman windows), which mitigate edge effects and improve the convergence of periodogram estimates (Percival & Walden, 1993). More fundamentally, transitioning from the spatial to the spectral domain changes the way spatial variability is conceptualized. Rather than examining variability by distance, frequency-domain analysis identifies dominant scales or periodicities in the data. In mineral exploration, this can highlight geological rhythms associated with lithological layering, cyclic magmatic events, or structurally controlled mineralization zones, often obscured in conventional variogram plots (Chilès & Delfiner, 2012). For instance, cyclic geochemical patterns caused by hydrothermal pulsations or rhythmic sedimentation may only be detectable in the frequency domain.

However, FT-based geostatistics also has notable limitations. Traditional FFT algorithms require data to lie on a regular grid, a condition seldom met in geochemical datasets from field exploration (Fuentes, 2007). While gridding or interpolation is possible, it introduces assumptions and potential inaccuracies. Moreover, aliasing where high-frequency signals appear as low-frequency due to under-sampling can distort interpretations. The Fourier Transform also assumes stationarity and infinite signal length, which rarely apply to real-world geoscientific data, causing spectral leakage and approximation errors

ISSN: 3043–6087. Science and Education Development Inst., Nigeria

(Priestley, 1981). To address these issues, several innovations have emerged. The Frequency Domain Empirical Likelihood (FDEL) method, for example, offers a non-parametric alternative suited to irregularly spaced data, avoiding direct variogram estimation and allowing distribution-free inference for spectral parameters (Bandyopadhyay et al., 2015). Another advancement is the weighted non-uniform Fourier sum, which introduces specialized weights to approximate Fourier integrals over irregularly spaced samples while minimizing aliasing and conditioning problems (Bajaj, 2013). These methods provide enhanced flexibility for modeling large and irregularly sampled geochemical datasets while preserving the diagnostic power of frequency-domain analysis. Ultimately, the FT reveals structural periodicities and large-scale controls on mineralization that would otherwise be hidden. In this context, Fourier-based geostatistical tools play a pivotal role in targeting exploration zones and improving geological interpretations based on spatial geochemical or geophysical signatures.

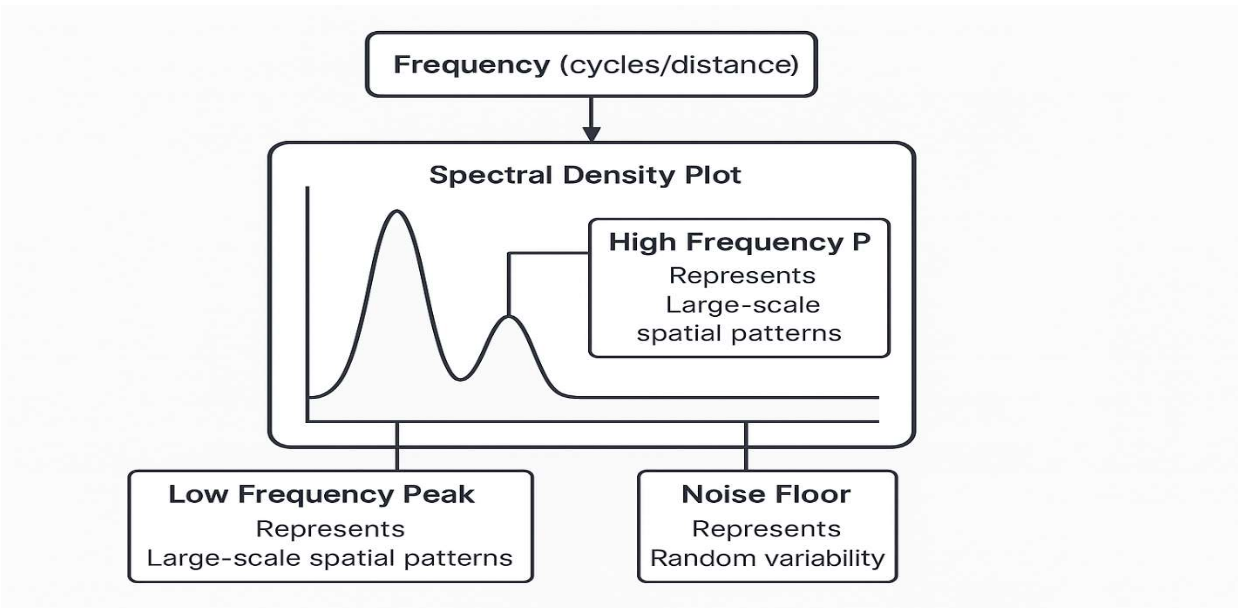

Figure 7: Conceptual Fourier Transform (Spectral Density) Plot. Peaks in the spectral density indicate dominant spatial frequencies or periodicities in the data, which can correspond to geological structures or processes operating at specific scales.

Wavelet Transform for Multi-Scale Anomaly Detection

The wavelet transform represents a significant advancement in spatial data analysis, particularly in geostatistics and mineral exploration. Developed in the 1980s, wavelet theory extends classical signal processing techniques by offering simultaneous

ISSN: 3043–6087. Science and Education Development Inst., Nigeria

localization in both space and frequency domains, enabling a more nuanced representation of spatial heterogeneity (Mallat, 1989). Unlike the Fourier Transform, which decomposes signals into global sine and cosine functions and is optimal for stationary signals, wavelet transforms decompose data into components that are localized in both scale and space. This makes wavelets exceptionally powerful for analyzing non-stationary signals and detecting localized anomalies (Percival & Walden, 2000).

Wavelets provide a multi-resolution analysis framework by filtering spatial data across several scales simultaneously. This capability allows for the detection of patterns that persist at specific scales or locations, thus capturing both broad trends and fine-scale irregularities in the data (Addison, 2002). For geostatistical applications, this means that wavelet transforms can identify features such as regional geochemical trends, intermediate-scale alteration halos, and small-scale ore-related anomalies within the same dataset. The wavelet transform's ability to filter out constant values and strong linear trends enhances its sensitivity to residual variation features that may correspond to subtle geochemical signatures of mineralization (Mahdiyanfar & Salimi, 2022; Liang, et al., 2023). A key advantage of wavelet transforms is their capacity to represent and manipulate spatial variability with minimal assumptions about data structure. Unlike traditional variograms, wavelets do not require stationarity or isotropy assumptions, making them robust in complex geological environments (Mallat, 1991). The global wavelet spectrum offers a summary of dominant variation scales across the dataset, while the wavelet transform itself can pinpoint the exact locations of anomalous features. This dual capability is crucial for mineral exploration, where identifying both regional metallogenic trends and discrete ore bodies is critical. Moreover, wavelet coherency analysis allows for the exploration of scale-specific and location-specific relationships between different geochemical variables (Grinsted et al., 2004). For instance, it can reveal how trace element enrichment varies with lithological boundaries at certain scales, or how structural features influence mineral dispersion at multiple levels. These insights can significantly enhance geochemical modeling and anomaly detection.

Wavelets have also shown utility in multivariate geochemical analysis. When applied to high-dimensional datasets, such as those from portable XRF or ICP-MS, wavelet transforms help reduce data dimensionality while preserving meaningful geochemical structure (Günaydın & Şen, 2025). This is especially useful in environments with overlapping geochemical signatures from multiple mineralizing processes. Wavelet-based filtering techniques have been used in conjunction with calibration models for spectral data, offering improved signal extraction and reduced noise in complex datasets (Jouan-Rimbaud et al., 1997; Cai et al., 1998). In practical applications, wavelet transforms

ISSN: 3043–6087. Science and Education Development Inst., Nigeria

support both grassroots and advanced-stage mineral exploration. At a regional scale, they help delineate geochemical provinces and identify metallogenic belts. At the deposit scale, they enhance the detection of alteration halos, zoning patterns, and ore controls, even in environments with complex background variation. This multi-scale analytical framework is increasingly recognized as essential for targeting in Greenfield exploration and improving deposit models in brownfield contexts (Li & Oldenburg, 2010; Kalkhoran, et al., 2025). The wavelet transform (Figure 8) offers a transformative approach to spatial data analysis, enabling geoscientists to explore the full spectrum of geochemical variability across scales and locations. Its application to mineral exploration allows for a more refined understanding of spatial patterns, ultimately improving anomaly detection, reducing false positives, and guiding efficient resource allocation in exploration campaigns.

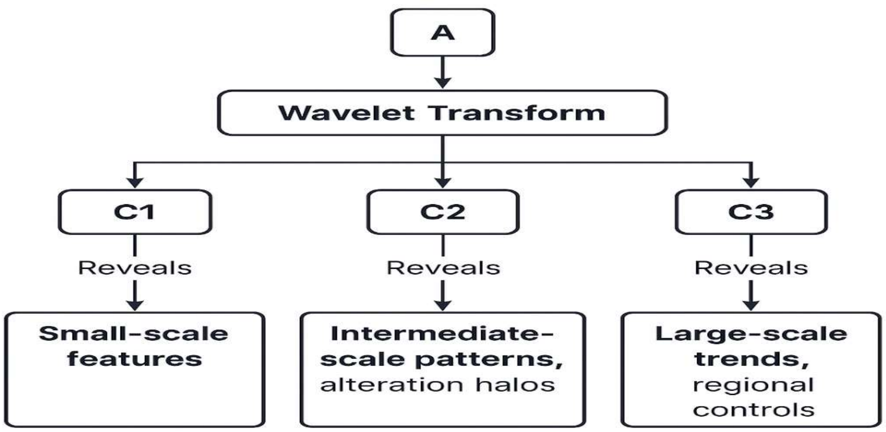

Figure 8: Conceptual Wavelet Decomposition of a Geochemical Signal. Wavelets break down the signal into different scales, allowing for the identification of both localized anomalies and broader spatial patterns, which is highly beneficial for multi-scale mineral exploration targeting.

Other Integral Transforms

Integral transforms are powerful mathematical tools that facilitate the transformation of complex functions into a more manageable form, typically by integrating the original function against a kernel function over a given domain (Debnath & Bhatta, 2014). These transforms simplify differential or integral equations into algebraic equations in a transformed domain, where solutions are often easier to obtain. Once a solution is derived in this new domain, an inverse transform is applied to retrieve the solution in the original space (Sneddon, 1972).

ISSN: 3043–6087. Science and Education Development Inst., Nigeria

Among these, the Laplace transform stands out as a classical method widely used in physics and engineering. It effectively converts differentiation and integration operations into multiplication and division within the Laplace (complex frequency) domain (Brown & Churchill, 2009). This characteristic makes it particularly useful for solving linear time-invariant differential equations and modeling dynamic systems. Despite their broad utility in applied mathematics and engineering, integral transforms such as the Laplace transform are not commonly used for empirical data transformation in geostatistics or variogram modeling. Unlike Fourier and wavelet transforms, which are tailored for analyzing frequency content and spatial scale in spatially distributed datasets, Laplace transforms are more suited to theoretical modeling of underlying physical processes (Isaaks & Srivastava, 1989). For instance, Laplace and related transforms are better utilized in solving partial differential equations governing heat flow or fluid migration in subsurface geology, rather than directly analyzing spatial variability in geochemical or geological datasets.

Thus, while integral transforms are invaluable for understanding the theoretical behavior of spatial processes, their direct application in variogram estimation or cross-variogram modeling remains limited. In contrast, wavelet and Fourier transforms directly address the multi-scale nature and frequency characteristics of spatial datasets, making them more appropriate for empirical geostatistical analysis and mineral exploration tasks (Chilès & Delfiner, 2012).

5. Application to Riruwai Geochemical Data: A Conceptual Framework for Mineral Exploration

The application of integral transform-based geostatistical methods to the Riruwai granitic complex in northern Nigeria offers an innovative approach to characterizing spatial relationships within geochemical datasets. Figure 9 illustrates a comprehensive geostatistical workflow incorporating integral transforms for mineral exploration. The central goal of this methodology is to leverage advanced data transformation techniques to improve the detection and interpretation of mineralization-related geochemical patterns. The process begins with rigorous data preprocessing outlier detection, compositional closure correction, and transformation of skewed variables. Due to the inherent skewness and heteroscedasticity in geochemical datasets, particularly in granite-hosted systems, Normal Score Transformation (NST) is employed to normalize the distributions. NST maps data to a standard normal distribution while preserving the rank order, enhancing the suitability of the dataset for linear geostatistical modeling such as variogram analysis (Goovaerts, 1997; Deutsch & Journel, 1998).

Elemental pair selection for cross-variogram modeling is guided by both geological reasoning and statistical association. For instance, SiO_2–Al_2O_3 may reflect alteration processes; Fe_2O_3–MgO could indicate mafic mineral enrichment; Cr–Ni might suggest ultramafic affinity or sulfide mineralization; Sr–Ba is linked to feldspar fractionation; and U–Th relates to radioactive enrichment often associated with REE-bearing systems (Rollinson, 1993; Möller, 1989; Olasehinde et al., 2025). These pairs are carefully selected to uncover spatial co-regionalization patterns relevant to granite-related mineral deposits. Following transformation, experimental cross-variograms are computed for these elemental pairs. Variogram modeling involves fitting theoretical models (e.g., spherical or exponential) to the empirical semivariances (Figure 10) calculated at various lags and directions (Journel & Huijbregts, 1978). The fitting provides estimates for nugget, sill, and range, which are key to understanding spatial continuity. Since the variograms are computed in transformed space, a back-transformation is applied to return estimates to the original units, ensuring meaningful interpretation for resource estimation (Goovaerts, 1997).

If the exploratory data analysis suggests underlying periodic or multi-scale patterns possibly related to magmatic pulses, structural controls, or hydrothermal fronts then Fourier or Wavelet Transforms can be incorporated. Fourier Transforms, which decompose data into spectral frequencies, are ideal for identifying dominant spatial periodicities that might be missed by standard variograms (Cheng, 2015; Wu, et al 2020; Heidari et al., 2021). However, their effectiveness is constrained by irregular sampling in geochemical datasets, such as those from Riruwai. To mitigate this, methods like weighted non-uniform Fourier sums or Frequency Domain Empirical Likelihood (FDEL) offer more flexible spectral estimation for irregularly spaced data (Cheng, 2018; Fuentes, 2007; Stein, 2007). On the other hand, wavelet transforms offer localized multi-scale decomposition and are less sensitive to sampling irregularity (Holden, et al., 2008; Torrence & Compo, 1998; Mahdiyanfar & Salimi, 2022; Liang et al., 2023). This capability allows for the detection of localized geochemical anomalies potentially small ore bodies or alteration zones and regional-scale patterns such as magmatic zonation or hydrothermal overprints (Figure 11). For instance, wavelet coherence analysis can reveal the co-variation of elements like Th and U at different scales and locations, which may highlight REE-enriched zones or potential uranium-bearing targets (Addison, 2017).

ISSN: 3043–6087. Science and Education Development Inst., Nigeria

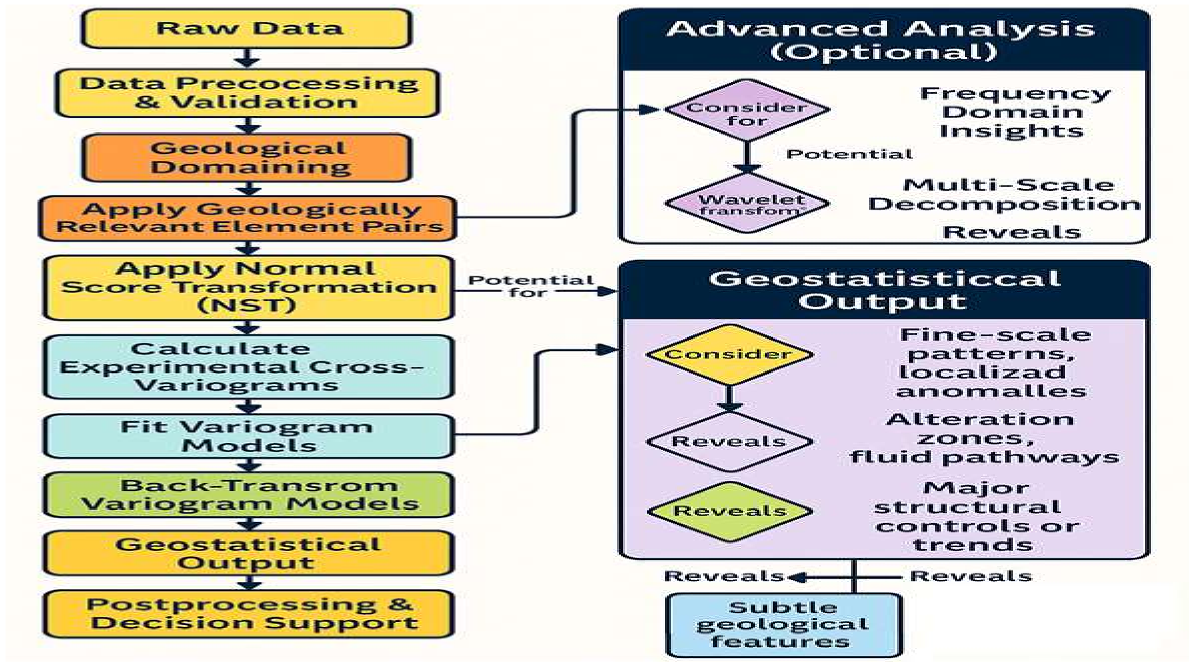

Figure 9: Integrated Geostatistical Workflow for Mineral Exploration. This workflow emphasizes data preprocessing, domaining, and the application of Normal Score Transformation for robust variogram modeling. Optional Fourier and Wavelet Transforms provide additional insights into structural controls and multi-scale anomalies, all contributing to improved resource estimation and exploration targeting.

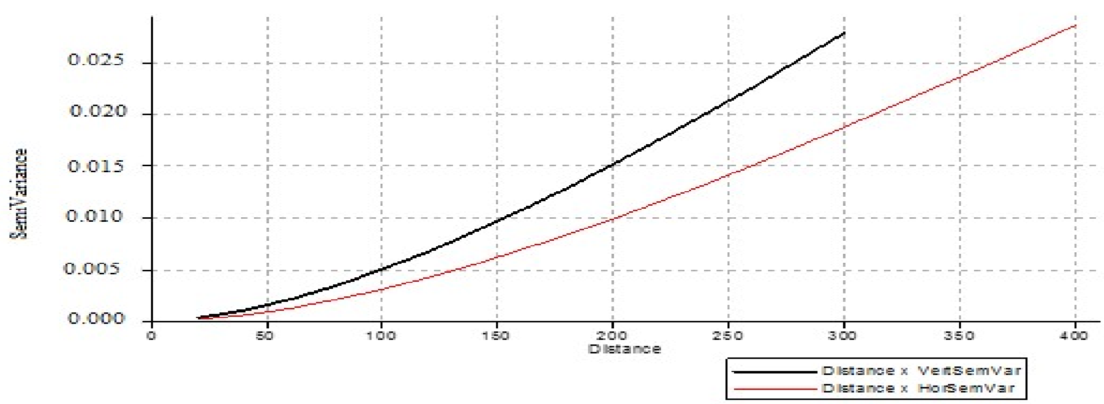

Figure 10. The semivariogram plot showing both ***Vertical (VertSemVar)*** *and* ***Horizontal (HorSemVar)*** *spatial variability*

ISSN: 3043–6087. Science and Education Development Inst., Nigeria

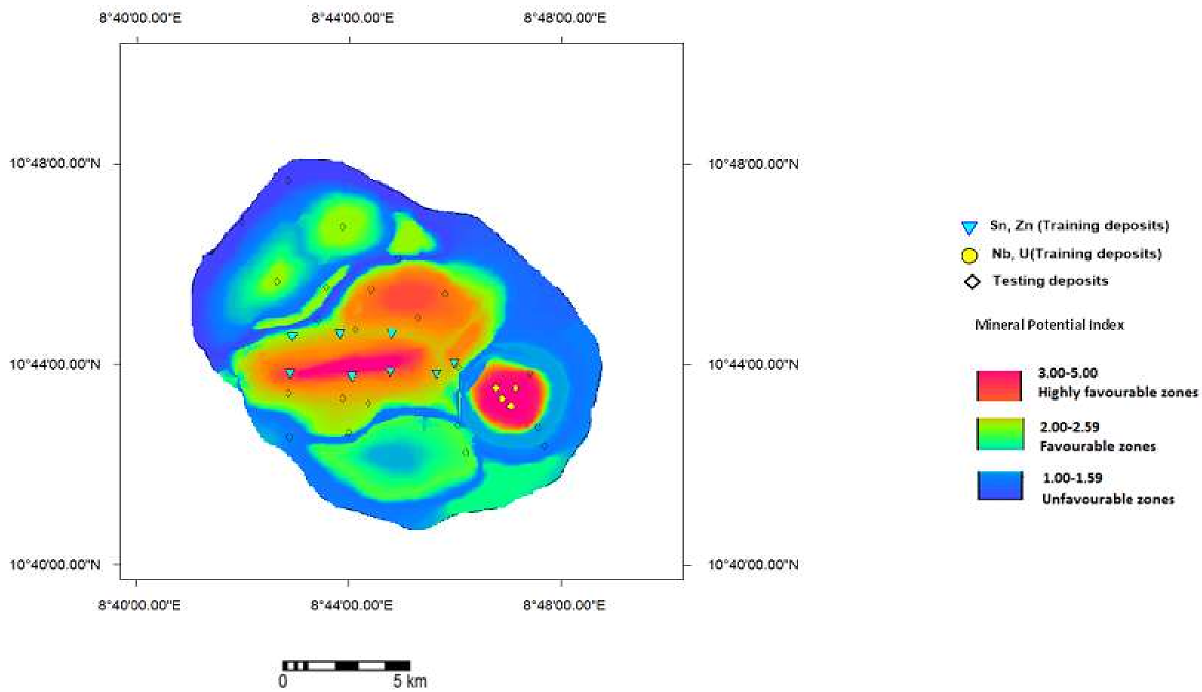

Figure 11. Mineral Potential Map of Riruwai Signifies increases in Alteration within the Lithology especially within the Granitic Areas due to Hydrothermal Alteration

6. Conclusions and Implications for Mineral Exploration

The application of integral transform approaches to cross-variogram modeling of geochemical data presents a sophisticated, yet practical framework for unraveling complex spatial interrelationships inherent in geological systems. In mineral exploration, where understanding the spatial distribution and co-regionalization of geochemical elements is critical, these methods offer a significant advancement over conventional techniques (Carranza, 2009; Cheng et al., 2011). Cross-variogram analysis, in particular, enables the quantification of spatial co-dependence between two or more geochemical variables, offering insights into the multivariate nature of mineralizing processes (Goovaerts, 1997; Wackernagel, 2003).

Among the suite of available transforms, the **Normal Score Transformation (NST)** stands out as a vital tool. Geochemical datasets are frequently non-Gaussian, characterized by skewness, heavy tails, and outliers, which can severely distort experimental variogram structures if left untreated. The NST mitigates these issues by transforming the data into a Gaussian distribution, making the statistical assumptions of variogram modeling and kriging more valid (Deutsch & Journel, 1998). While variogram parameters estimated in the transformed domain tend to be optimistic and must be back-transformed to yield realistic estimations, this transformation allows for more stable and interpretable model fitting, especially in the presence of extreme values (Gribov & Krivoruchko, 2004).

Fourier and Wavelet Transforms provide complementary capabilities. The Fourier Transform, by converting spatial data into the frequency domain, can detect hidden periodicities, revealing regional-scale structures or lithological patterns that influence mineralization (Chiles & Delfiner, 2012; Prieto et al., 2009). However, standard implementations are limited by the assumption of regular gridding a condition rarely met in geological surveys. This limitation necessitates the use of more flexible techniques such as the weighted nonuniform Fourier sum (Omre & Halvorsen, 1989) or Frequency Domain Empirical Likelihood (FDEL) (Molanes-López, et al., 2010), which can handle irregular spatial sampling, albeit with increased computational complexity.

Meanwhile, Wavelet Transforms enable the decomposition of geochemical signals into multiple spatial scales, allowing geoscientists to simultaneously analyze both local anomalies and regional trends. Their utility is particularly pronounced in environments with overlapping geological features or superimposed mineralization events, such as the Riruwai Younger Granite Complex, where granitic, hydrothermal, and structural controls converge (Kinnaird et al., 1985; Ogunleye, et al., 2006; Girei et al., 2019; Olasehinde et al., 2012; Olaehinde et al., 2025). By identifying localized variations and filtering out noise or large-scale trends, wavelets enhance the resolution of geochemical zoning and support more precise target delineation (Gyozo & Bertram, 2005; Mahdiyanfar, & Seyedrahimi-Niaraq, 2024).

In the case of the Riruwai geochemical dataset, the integration of these integral transform techniques into a geostatistical workflow proved invaluable. Following domain-based preprocessing and selection of pathfinder elements, NST was applied to reduce the influence of skewness. Cross-variograms of transformed data were calculated for key elemental pairs such as Fe_2O_3–MgO and U–Th and theoretical models were fitted. The resulting model parameters, once back-transformed, yielded improved representations of spatial continuity and co-regionalization. These models not only highlighted areas of enhanced mineral potential but also helped delineate the spatial extent of alteration zones and magmatic differentiation processes. Furthermore, they identified anomalous geochemical signatures that deviate from regional trends, potentially indicating undiscovered mineralization or zones of hydrothermal overprinting.

Overall, integral transform approaches particularly when tailored to the data's characteristics and geological context offer powerful tools for enhancing the robustness and interpretability of geostatistical models. The successful application of such methods demands a balanced integration of quantitative rigor and geological reasoning. When executed appropriately, this synergy enhances spatial prediction accuracy, supports more reliable resource estimation, and reduces exploration risk. As such, integral transforms are poised to play an increasingly central role in the geoscientific toolkit, particularly for the nuanced demands of modern mineral exploration.

References

Addison, P. S. (2002). The illustrated wavelet transform handbook: Introductory theory and applications in science, engineering, medicine and finance. CRC Press.

Addison, P. S. (2017). The illustrated wavelet transform handbook (2nd ed.). CRC Press.

Bajaj, C., Bauer, B., Bettadapura, R., & Vollrath A. (2013). Nonuniform Fourier transforms for rigid-body and multi-dimensional rotational correlations. *SIAM J Sci Comput.* 1;35(4):10.1137/120892386. doi: 10.1137/120892386

Bandyopadhyay, S., Lahiri, S. N., & Nordman, D. J. (2015). A frequency domain empirical likelihood method for irregularly spaced spatial data. *The Annals of Statistics*, *43*(2), 519–545. http://www.jstor.org/stable/43556526

Boisvert J.B., & Deutsch C.V. (2011) Programs for kriging and sequential Gaussian simulation with locally varying anisotropy using non-Euclidean distances. Computers & Geosciences 37(4): 495–510

Bracewell, R. N. (2000). The Fourier transform and its applications (3rd ed.). McGraw-Hill.

Briggs, W. L., & Henson, V. E. (1995). The DFT: An owner's manual for the discrete Fourier transform**.** SIAM.

Brown, J. W., & Churchill, R. V. (2009). *Complex variables and applications*. (8th ed.). New York: McGraw-Hill.

Cai, C., & Harrington, P. D. B. (1998). Different discrete wavelet transforms applied to denoising analytical data. *Journal of Chemical Information and Computer Sciences*, *38*(6), 1161-1170.

ISSN: 3043–6087. Science and Education Development Inst., Nigeria

Cameron, E. M., Hamilton, S. M., Leybourne, M. I., et al., Hall, G.E.M.,& McClenaghan, M.B. (2004). Finding Deeply Buried Deposits Using Geochemistry. *Geochemistry: Exploration, Environment, Analysis*, 4(1): 7–32. https://doi.org/10.1144/1467-7873/03-019

Carranza, E. J. M. (2009). Geochemical Anomaly and Mineral Prospectivity Mapping in GIS. *Handbook of Exploration and Environmental Geochemistry,* Volume 11. Elsevier, Amsterdam

Carranza, E. J. M. (2012). Geochemical characteristics of mineral deposits: Implications for ore genesis. *Geochemistry Exploration Environment Analysis.* 12. 89-92. 10.1144/1467-7873/12-MINDEP-122.

Cheng, Q., Bonham-Carter, G., Wang, W. L., Zhang, S., Li, W., & Qinglin, X. (2011). A Spatially Weighted Principal Component Analysis for Multi-Element Geochemical Data for Mapping Locations of Felsic Intrusions in the Gejiu Mineral District of Yunnan, China. *Computers & Geosciences*, 37(5): 662 669. https://doi.org/10.1016/j.cageo.2010.11.001

Cheng, Q. (2015). Multifractal interpolation method for spatial data with singularities. *Journal of the Southern African Institute of Mining and Metallurgy*, *115*(3), 235-240.

Cheng, Q. (2018). Mathematical geosciences: Local singularity analysis of nonlinear Earth processes and extreme geo-events. In *Handbook of Mathematical Geosciences: Fifty Years of IAMG* (pp. 179-208). Cham: Springer International Publishing.

Chilès, J. P., & Delfiner, P. (2012). Geostatistics: Modeling spatial uncertainty (2nd ed.). Wiley.

Cressie, N. A. C. (1993). Statistics for spatial data (2nd ed.). Wiley.

Debnath, L., & Bhatta, D. (2014). Integral transforms and their applications (3rd ed.). CRC Press.

Deutsch, C. V., & Journel, A. G. (1998). GSLIB: Geostatistical software library and user's guide (2nd ed.). Oxford University Press.

Frigo, M., & Johnson, S. G. (2005). The design and implementation of FFTW3. Proceedings of the IEEE, 93(2), 216–231. https://doi.org/10.1109/JPROC.2004.840301

ISSN: 3043–6087. Science and Education Development Inst., Nigeria

Fuentes, M. (2007). Approximate Likelihood for Large Irregularly Spaced Spatial Data. *Journal of the American Statistical Association*, *102*(477), 321–331. https://doi.org/10.1198/016214506000000852

Girei, M. B., Li, H., Algeo, T. J., Bonin, B., Ogunleye P. O., Bute, S. I., & Ahmed, H. A. (2019). Petrogenesis of a-type granites associated with Sn–Nb–Zn miniralisation in Ririwai complex, north-central Nigeria: Constraints from whole-rock Sm-Nd and zircon Lu-Hf isotope systematics. *Lithos* 340–341, 49–70

Goovaerts, P. (1997). Geostatistics for natural resources evaluation. Oxford University Press.

Gribov, A., & Krivoruchko, K. (2004). Geostatistical mapping with continuous moving neighborhood. *Mathematical Geology*, **36**(11), 267-281

Grinsted, A., Moore, J. C., & Jevrejeva, S. (2004). Application of the cross wavelet transform and wavelet coherence to geophysical time series. Nonlinear Processes in Geophysics, 11(5/6), 561–566.

Gyozo, J., & Bertram, S., (2005). Application of wavelet analysis to the study of spatial pattern of morphotectonic lineaments in digital terrain models. A case study. *Remote Sensing of Environment,* 94(1) 31-38, https://doi.org/10.1016/j.rse.2004.08.013.

Günaydın, Y. Ş., & Şen, B. (2025). A Multi-Scale Unsupervised Feature Extraction Network with Structured Layer-Wise Decomposition. Applied Sciences, **15**(13), 7194. https://doi.org/10.3390/app15137194

Heidari, S.M., Afzal, P., Ghaderi, M., Sadeghi, B (2021). Detection of mineralization stages using zonality and multifractal modeling based on geological and geochemical data in the Au-(Cu) intrusion-related Gouzal-Bolagh deposit, NW Iran, *Ore Geology Reviews,* 139, Part B, https://doi.org/10.1016/

Holden, E. J., Dentith, M., & Kovesi, P. (2008). Towards the automated analysis of regional aeromagnetic data to identify regions prospective for gold deposits. *Computers & Geosciences*, *34*(11), 1505-1513.

Isaaks, E. H., & Srivastava, R. M. (1989). An introduction to applied geostatistics. Oxford University Press.

Kinnaird, J. A., Bowden, P., Ixer, R. A., & Odling, N. W. A. (1985). Mineralogy, geochemistry, and miniralisation Ririwai complex, Northern Nigeria. *Journal Africa Earth. Science*, 3, 185-222.

Li, Y., & Oldenburg, D. W. (2010). Rapid construction of equivalent sources using wavelets. *Geophysics*, *75*(3), L51-L59.

Liang, Y., Xia, Q., Zhao, M., Bi, R., & Liu, J. (2023). Application and Significance of the Wavelet–Fractal Method on the Data of the Induced Polarization Method in the Graphite Deposits of Datong, China. *Minerals*, *13*(6), 760.

Jouan-Rimbaud, D., Walczak, B., Poppi, R. J., De Noord, O. E., & Massart, D. L. (1997). Application of wavelet transform to extract the relevant component from spectral data for multivariate calibration. *Analytical chemistry*, *69*(21), 4317-4323.

Journel, A. G., & Huijbregts, C. J. (1978). Mining geostatistics. Academic Press.

Jourdan, A. (2004). Multiscale analysis using wavelets for geochemical and geophysical mapping. Geochemistry: Exploration, Environment, Analysis, 4(3), 239–248.

Kalkhoran, S. E., Ghannadpour, S. S., & Pour, A. B. (2025). Optimized Hydrothermal Alteration Mapping in Porphyry Copper Systems Using a Hybrid DWT-2D/MAD Algorithm on ASTER Satellite Remote Sensing Imagery. *Minerals*, *15*(6), 626.

Lark, R. M. (2000). Estimating variograms of soil properties by the method-of-moments and maximum likelihood. European Journal of Soil Science, 51(4), 717–728.

Madani, N., Maleki, M., & Soltani-Mohammadi, S. (2022).Geostatistical modeling of heterogeneous geo-clusters in a copper deposit integrated with multinomial logistic regression: An exercise on resource estimation*, Ore Geology Reviews,150*,105132, https://doi.org/10.1016/j.oregeorev.2022.105132.

Mahdiyanfar, H., & Salimi, A. (2022). Fractal modeling of geochemical mineralization prospectivity index based on centered Log-Ratio transformed data for geochemical targeting: a case study of Cu porphyry mineralization. *Journal of Mining and Environment*, *13*(3), 821-838.

ISSN: 3043–6087. Science and Education Development Inst., Nigeria

Mahdiyanfar, H & Seyedrahimi-Niaraq, M. (2024). Application of Hybrid Wavelet-Fractal Approach for Denoising and Spatial Modeling of Environmental Pollution. *Journal of Mining and Environment* 15(4), 1579-1590

Mallat, S. (1989). A theory for multiresolution signal decomposition: The wavelet representation. **IEEE** Transactions on Pattern Analysis and Machine Intelligence, 11(7), 674–693.

Mallat, S. (1991). Zero-crossing of a wavelet transform. **IEEE** Transactions on Information Theory, 37(4), 1019–1033.

Matheron, G. (1965). Les variables régionalisées et leur estimation. Masson.

Molanes-López, E., Cao, R., & Keilegom, I. (2010). Smoothed empirical likelihood confidence intervals for the relative distribution with left-truncated and right-censored data. *Canadian Journal of Statistics.* 38. 453 - 473. 10.1002/cjs.10079.

Möller, P., (1989). Rare earth mineral deposits and their industrial importance, in Möller, Peter, Cerny, Petr, and Saupé, Francis, eds., Lanthanides, tantalum and niobium-- mineralogy, geochemistry, characteristics of primary ore deposits, prospecting, processing and applications: New York, SpringerVerlag, p. 171-188.

Myers, D. E. (1982). Matrix formulation of co-kriging. Mathematical Geology, 14(3), 249–257.

Ogunleye, P. O., Garba. I., & Ike, E. C. (2006). Factors contributing to enrichment and crystallization of niobium in pyrochlore in the Kaffo albite arfvedsonite granite, Ririwai Complex, Younger Granites province of Nigeria. *Journal of African Earth Sciences,* 44(3), 372-382.

Olasehinde, A., Ashano, E.C., and Singh, G.P. (2012). Analysis of Magnetic Anomaly over the Riruwai Younger Granite Complex: A Geodynamic Implication. *Cont. J. Earth. Sci. Vol 7(1) pp 9-18*

Olasehinde , A., Mohammed, A.G., Daspan, R.I and Ashano, E.C (2025). Geochemical Characterization and Mineralization Potential of Kaffo Albite Arfvedsonite Granites in the Riruwai Younger Granite Complex, Nigeria. *Dutse Journal of Pure and Applied Sciences (DUJOPAS).* 11(1c). 347-358

Omre, H., & Halvorsen, K. B. (1989). The Bayesian bridge between simple and universal kriging. *Mathematical Geology*, 21 (7) 767–786.

Percival, D. B., & Walden, A. T. (1993). Spectral analysis for physical applications: Multitaper and conventional univariate techniques**.** Cambridge University Press.

Percival, D. B., & Walden, A. T. (2000). Wavelet methods for time series analysis. Cambridge University Press.

Perret, J., André-Mayer, A., Eglinger, A., Feneyrol, J., Voinot, A., Morlot, C., Barou, F., Teitler, Y., Seira, D., & Bosc, R. (2021). Structural and geochemical ore-forming processes in deformed gold deposits: towards a multi-scale and -method approach. *Geological Society London Special Publications.* 516. 10.1144/SP516-2021-37.

Priestley, M. B. (1981). *Spectral analysis and time series* (Vol. 1). Academic Press.

Prieto, G. A., Parker, R. L., & Vernon, F. L. (2009). A Fortran 90 library for multitaper spectrum analysis. Computers & Geosciences, 35, 1701–1710.

Reimann, C., & Filzmoser, P. (2000). Normal and lognormal data distribution in geochemistry: Death of a myth. Consequences for the statistical treatment of geochemical and environmental data. Environmental Geology, 39(9), 1001–1014. doi:10.1007/s002549900081

Rollinson, H. (1993). Using geochemical data: Evaluation, presentation, interpretation**.** Wiley, New York.

Sneddon, I. N. (1972). The use of integral transforms**.** New York. McGraw-Hill.

Stein, M. L. (2007). Spatial variation of total column ozone on a global scale. The Annals of Applied Statistics, 1(1), 191–210.

Thayer,W.C., Griffith, D.A., Goodrum, P.E., Diamond, G.L., & Hassett, J.M. (2003). Application of geostatistics to risk assessment. Risk Anal. 23(5), 945-60. doi: 10.1111/1539-6924.00372.

Torrence, C., & Compo, G. P. (1998). A practical guide to wavelet analysis. Bulletin of the American Meteorological Society, 79(1), 61–78.

Verly, G.W. (1993) Sequential Gaussian Cosimulation: A Simulation Method Integrating Several Types of Information. In: Verly, G.W., Ed., Sequential Gaussian Cosimulation: A Simulation Method Integrating Several Types of Information. *Geostatistics Troia* 1, 543-554. https://doi.org/10.1007/978-94-011-1739-5_42

Wackernagel, H. (2003). Multivariate geostatistics: An introduction with applications (3rd ed.). Springer.

Wang, Z., Li., Y., & Wang, J.G. (2007). A damage-softening statistical constitutive model considering rock residual strength, Computers & Geosciences, (33)1, 1-9, https://doi.org/10.1016/j.cageo.2006.02.011

Wu, R., Chen, J., Zhao, J., Chen, J., & Chen, S. (2020). Identifying Geochemical Anomalies Associated with Gold Mineralization Using Factor Analysis and Spectrum–Area Multifractal Model in Laowan District, Qinling-Dabie Metallogenic Belt, Central China. Minerals**,** 10(3), 229. https://doi.org/10.3390/min10030229